Low-Temperature Solution Synthesis of Chemically Functional Ferromagnetic FePtAu Nanoparticles

Sachin Kinge,*,†,‡,§ Tian Gang,†,‡ Wouter J. M. Naber,‡ Hans Boschker,‖ Guus Rijnders,‖ David N. Reinhoudt,§ and Wilfred G. van der Wiel*,‡

Strategic Research Orientation NanoElectronics, Laboratory of Supramolecular Chemistry and Technology, Faculty of Science and Technology, and Inorganic Materials Science Group, Faculty of Science and Technology, MESA+ Institute for Nanotechnology, University of Twente, 7500 AE Enschede, The Netherlands

ABSTRACT

Magnetic nanoparticles are of great scientific and technological interest. The application of ferromagnetic nanoparticles for high-density data storage has great potential, but energy efficient synthesis of uniform, isolated, and patternable nanoparticles that remain ferromagnetic at room temperature is not trivial. Here, we present a low-temperature solution synthesis method for FePtAu nanoparticles that addresses all those issues and therefore can be regarded as an important step toward applications. We show that the onset of the chemically ordered face-centered tetragonal ($L1_0$) phase is obtained for thermal annealing temperatures as low as 150 °C. Large uniaxial magnetic anisotropy (10^7 erg/cm^3) and a high long-range order parameter have been obtained. Our low-temperature solution annealing leaves the organic ligands intact, so that the possibility for postanneal monolayer formation and chemically assisted patterning on a surface is maintained.

The continuously increasing demand for data storage capacity has very much stimulated research on magnetic recording media.[1,2] In modern hard disk drives, the magnetic medium layer is usually a CoCr-based alloy, containing submicrometer magnetic regions representing the bits of information. Every single magnetic region consists of ~100 magnetic grains, which are the basic elements to be magnetized. One of the main challenges in increasing the data storage capacity by reducing the magnetic grain size is maintaining its magnetization despite the superparamagnetic limit.[3-6] Current hard disk technology has an estimated limit of 100−1000 gigabit per square inch due to this superparamagnetic limit.[1,2]

It has been argued[1,2] that thin layers (ideally *monolayers*) of ferromagnetic FePt nanoparticles (NPs) enable recording densities ~10 times larger than those achievable with CoCr-based media. Due to their very high magnetocrystalline anisotropy ($K_u = 10^7$ erg/cm^3), FePt NPs remain ferromagnetic up to room temperature, even for few nanometer particle sizes. Furthermore, in traditional magnetic media, grain sizes show a wide distribution in size and shape,

reducing the signal-to-noise ratio. In contrast, FePt NPs can be chemically synthesized with a highly uniform shape and narrow size distribution.[1,2] This ultimately allows for 1 bit per nanometer-sized grain storage capacity.[7]

One of the major issues in FePt NP growth, however, is the need for a high-temperature annealing treatment (~700 °C and above) to obtain the desired high magnetocrystalline anisotropy.[8] The as-synthesized FePt NPs are namely in the chemically disordered face-centered-cubic (fcc) phase, which has low magnetic anisotropy. High-temperature annealing converts the NPs into the chemically ordered face-centered-tetragonal (fct) phase, referred to as the $L1_0$ phase, where Fe and Pt planes alternate along the *c*-axis. High-temperature annealing, however, has a couple of severe disadvantages. Annealing is usually performed on dried nanopowders, which often results in particle agglomeration and, consequently, a reduction of the particle uniformity and magnetic anisotropy. High-temperature annealing also destroys the organic ligands of the NPs, which takes away the advantage of the specific chemical functionality of the end groups, useful for chemical recognition and self-assembly in monolayers. A couple of methods have been developed to avoid agglomeration upon annealing, including a thick (10 nm) SiO$_2$ coating,[9] salt matrix annealing,[10] zeolite matrix annealing,[11] and quite recently MgO coating.[12,13] Although these methods reduce agglomeration and result in ferromagnetic NPs at room

* To whom correspondence should be addressed. Current E-mail: sachin.kinge@toyota-europe.com; W.G.vanderWiel@utwente.nl.
† These authors contributed equally to this work.
‡ Strategic Research Orientation NanoElectronics, MESA+ Institute for Nanotechnology.
§ Laboratory of Supramolecular Chemistry and Technology, Faculty of Science and Technology.
‖ Inorganic Materials Science Group, Faculty of Science and Technology.

temperature, still high temperatures are required and consequently the organic ligands are destroyed, losing all chemical functionality.

Given the above problems, a reduced annealing temperature is strongly favored. Doping the FePt lattice with specific transition metals turns out to be advantageous for the $L1_0$ phase transformation.[1,2,14] Au (or Ag) doping in small amounts leads to significant lowering of the annealing temperature for transforming the face-centered cubic (fcc) phase to the fct $L1_0$ phase. This is suggested to be related to defects and strain introduced by Au (or Ag) atoms. Upon annealing, Au (or Ag) atoms leave the FePt lattice at low temperature, leaving lattice vacancies that increase the mobility of Fe and Pt atoms to rearrange.[3−6,14] Dry annealing studies of FePtAu NPs show a lowering of the annealing temperature with at least 100 °C compared to FePt NPs.[3−6,14] Although dry annealing at reduced annealing temperatures results in (partly) transformation into the $L1_0$ phase, still large-scale NP agglomeration occurs.[15−17] A way to avoid this is to anneal the NPs in a liquid. Harrell et al. investigated postsynthesis, high-pressure annealing of FePtAu NPs in diphenyl ether solvent, and in silicone oil at atmospheric pressure.[14] However, these methods result in significant increase in particle size. Alternatively, one can already perform the NP synthesis at elevated temperature in a high-boiling point solution. This was done by Jia et al., improving somewhat the dispersity.[18]

Here, we present a comprehensive and systematic study of low-temperature, solution synthesis that results in highly uniform ferromagnetic and chemically patternable FePtAu NPs. Magnetic analysis indicates a large $L1_0$ phase fraction and that NPs of few nanometer size remain ferromagnetic up to room temperature. The onset for the $L1_0$ phase occurs for annealing temperatures as low as 150 °C, where the long-range order parameter S[16] increases monotonically with annealing temperature. Importantly, we find that our procedure leaves the organic ligands intact and demonstrates postanneal chemically assisted monolayer patterning. We thus synergistically combine inorganic (magnetic) and organic materials, as well as bottom-up (self-assembly) and top-down fabrication methods, being main motivations for organic spintronics.[19]

Our FePtAu NP synthesis is partly based on that of Jia et al.;[18] see Supporting Information. To synthesize FePtAu NPs, we use a combination of oleic acid and oleyl amine as stabilizing agent. The preparation is based on the reduction of platinum acetylacetonate and gold acetate by a diol and the decomposition of iron pentacarbonyl in high-temperature solutions. The octyl ether and hexadecylamine are used as solvents. Importantly, the addition of octyl ether as a solvent is different from the original method described by Jia et al. and is considered essential in our case. Hexadecylamine is solid, whereas octyl ether is liquid at room temperature. This allows the metal precursors already to dissolve at low temperature in the octyl ether before the hexadecylamine becomes liquid. We expect that our improved mixing conditions are responsible for the small size dispersity for our NPs.
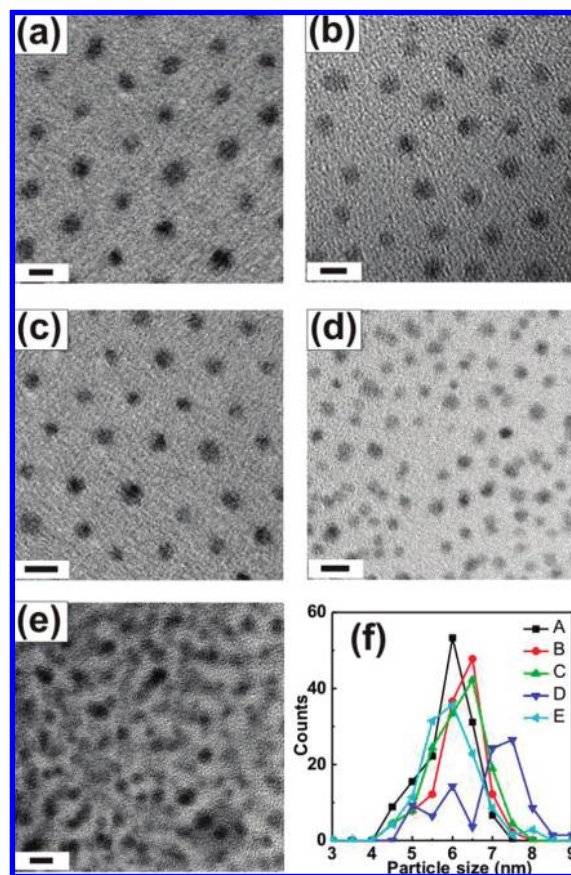
Figure 1. TEM images of $(FePt)_{85}Au_{15}$ NPs synthesized under different conditions: (a) 150 °C, 30 min; (b) 150 °C, 3 h; (c) 200 °C, 3 h; (d) 250 °C, 3 h; (e) 350 °C, 3 h. Scale bars correspond to 10 nm. (f) Particle size distribution determined from TEM images. Curves A−E correspond to panels a−e, respectively.

Figure 1 shows transmission electron microscope (TEM) images of $(FePt)_{85}Au_{15}$ NPs synthesized at standard conditions (30 min at 150 °C, Figure 1a), and for 3 h at 150−350 °C (Figure 1, parts b−e, respectively). The TEM analysis indicates regular NP assembly and small size dispersion, in particular for the lowest synthesis temperatures (Figure 1f).

The particle diameters for different synthesis temperatures, derived from TEM analysis, and the elementary composition of the particles obtained from energy dispersive X-ray diffraction (EDX) are given in Table 1. At 250 and 350 °C, the NPs have a broader size distribution. For synthesis at 150 and 200 °C, the average NP composition is uniform and close to the metal precursor ratio. At 250 and 350 °C a relative large distribution of Au contents is observed. NPs with Au content as high as $Fe_{16}Pt_{22}Au_{62}$ and as low as $Fe_{47}Pt_{45}Au_8$ are observed for 250 °C. For 350 °C the highest Au content was $Fe_{21}Pt_{24}Au_{55}$ and lowest $Fe_{41}Pt_{47}Au_{12}$. This suggests the segregation of Au atoms from the FePt bulk at higher temperatures. This is in agreement with the mechanism suggested above that Au creates empty sites, which can subsequently be occupied by randomly distributed Fe and Pt atoms, thereby transferring the fcc disordered phase into the ordered fct ($L1_0$) phase.[3−6,14]

Figure 2 shows the XRD analysis, indicating the evolution of the $L1_0$ phase with increasing synthesis temperature. The

Table 1. Summary of TEM Particle Sizes and Lattice Parameters Calculated from XRD Analysis

sample	synthesis temp (°C)	synthesis time (h)	diameter (nm)(TEM)	particle composition (EDX)	lattice constant (Å) (XRD) [111]
A	150	0.5	5.5 ± 0.3	$Fe_{42}Pt_{41}Au_{17}$	2.294
B	150	3	6.2 ± 0.3	$Fe_{42}Pt_{44}Au_{14}$	2.262
C	200	3	6.4 ± 0.3	$Fe_{42}Pt_{40}Au_{18}$	2.241
D	250	3	7.2 ± 0.3	distributed	2.234
E	350	3	5.8 ± 2.3	distributed	2.211
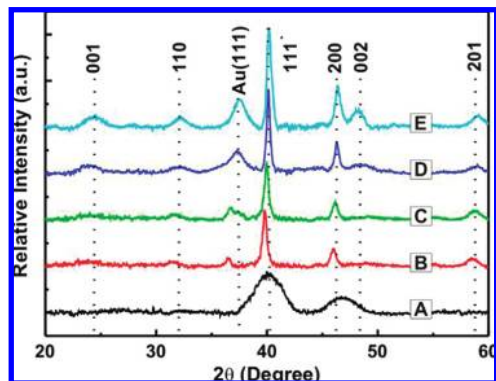
Figure 2. XRD spectra of $(FePt)_{85}Au_{15}$ NPs: 150 °C, 30 min (A); 150 °C, 3 h (B); 200 °C, 3 h (C); 250 °C, 3 h (D); 350 °C, 3 h (E).

evolution of the superlattice peaks, (001) and (110), as well as the fundamental peak (002), is clearly observed. The development of the Au(111) peak indicates the segregation of Au atoms from the FePt fcc lattice thereby transforming the lattice to fct ($L1_0$).

The lattice constant determined from the Pt(111) peak indicates a gradual decrease from 2.262 Å (150 °C, 3 h) to 2.211 Å (350 °C, 3 h), see Table 1, slowly approaching the ideal value of 2.197 Å for a FePt fct lattice. The as-synthesized particles (150 °C, 30 min.) show a lattice constant of 2.294 Å, indicating a fcc lattice. This clearly demonstrates the phase transformation from fcc to fct NPs.

To quantify the chemical ordering in the $L1_0$ phase, one often uses the long-range ordering parameter S, defined as[20]

$$S \cong 0.85 \left(\frac{I_{001}}{I_{002}} \right)^{1/2} \qquad (1)$$

where I_{001} and I_{002} are the integrated intensities of the superlattice 001 and fundamental 002 peaks in the XRD spectrum. S is unity for perfectly ordered films and is zero for a chemically disordered film.[21] The long-range order parameter S for different synthesis temperatures extracted from the XRD data is plotted in Figure 3d (open symbols). The ordering parameter linearly increases with synthesis temperature, reaching $S = 0.68$ for 350 °C. For comparison, Sun et al. have achieved an ordering parameter of $S = 0.98$ for dry annealing at 725 °C for 2 h in He.[1,2] Here we achieve significant ordering without much agglomeration at temperatures not more than 350 °C, maintaining the end group functionality (see below). The ordering process starts already from 150 °C onward for longer synthesis times. This is very remarkable as previous reports for annealed NP powders showed the onset of ordering around 350 °C (30 min).[3−6,14]

As suggested by Chepulskii et al., the ordering process is kinetically regulated.[17,22] As a consequence, it is expected that approaching the equilibrium ordered state at low temperature will take longer. Therefore kinetic acceleration methods such as irradiation and or addition of other types of atoms are potentially effective in accelerating the formation of long-range order. To the best of our knowledge, all the previous studies report the synthesis of NPs by refluxing the precursor's solution only for 30 min. Here, we have increased the duration of gentle refluxing to 3 h. Increasing the refluxing time gives the NPs more time to organize in the desired crystal phase (kinetic control). This results in significantly higher chemical ordering of our NPs in the fct phase.

X-ray photoelectron spectroscopy (XPS) is performed to analyze the elemental states of Fe, Pt, and Au in the NPs (See Supporting Information) The NP surface composition indicates the presence of Fe_2O_3, while removal of the outer 1 nm shell by sputtering results in a composition of elements near to the expected value. This suggests that the surface is partially covered with Fe_2O_3.

We have prepared single monolayers of FePtAu NPs for magnetic characterization.[2,21] A silicon/silicon oxide substrate is functionalized with a very thin polyethylenimine (PEI) layer. When the polymer−derivative substrate is dipped into the particle dispersion, pendant functional groups of the polymer replace the particle stabilizers and a strong monolayer particle assembly is formed. The substrate is then rinsed with solvent to remove physical sorption and dried. This process results in one single FePtAu NP monolayer.

The magnetic properties of NP monolayers are characterized by a vibrating sample magnetometer (VSM) with variable temperature insert (5−300 K). The magnetization curves at 5 and 300 K for NPs synthesized at different temperatures are shown in parts a and b of Figure 3, respectively. The coercive field (H_c) clearly increases with synthesis temperature. At 5 K, magnetic hysteresis is observed for all synthesis temperatures, whereas at 300 K hysteresis is observed for synthesis temperatures 200 °C ($H_c = 600$ Oe), 250 °C ($H_c = 2700$ Oe), and 350 °C ($H_c = 4800$ Oe). This demonstrates room-temperature ferromagnetism from synthesis temperatures starting from 200 °C only.

The saturation magnetic moment of our monolayers is ∼35−40 μemu, both at room temperature and low temperature. We compare this value for 350 °C synthesis temperature with the momentum density of bulk FePt (1140 emu/cm^3),[23] assuming the ratio of FePt in our FePtAu NPs to be 0.85, 2.9 nm NP radius, and 1 nm ligand length. On the basis of those parameters, we find (see Supporting Information) a saturation magnetic moment of 47 μemu. The experimentally
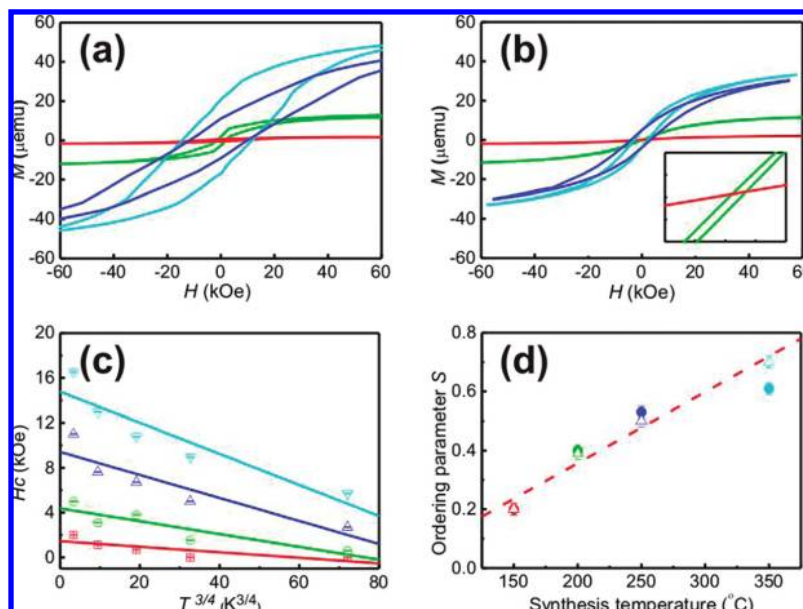
Figure 3. NP magnetization curves for different synthesis conditions measured by VSM at 5 K (a) and at room temperature (b). The inset of (b) is a zoom-in around zero field. The horizontal and vertical axis ranges are 0.5 kOe and 0.2 μemu, respectively. In all figures, the curve color refers to the different synthesis conditions: red 150 °C, 3 h; green 200 °C, 3 h; blue 250 °C, 3 h; cyan 350 °C, 3 h. H_c versus $T^{3/4}$ plots, used for fitting to the Garcia-Otero model, see text (c). Ordering parameter S, extracted from XRD data (open triangles) and H_c versus $T^{3/4}$ plots (solid dots), respectively, versus synthesis temperature (d). The linear dashed line is a guide to the eye.

observed value is slightly lower, as expected when taking into account the not fully developed L1$_0$ phase and lower effective packing density.

The observed temperature dependence of our magnetic hysteresis loops can be understood by realizing that the NP coercive fields decrease due to thermal fluctuations at the temperature increases. In this regard, Sharrock's formula[24] is the most widely used thermal relaxation model. However, it is valid for 2D systems rather than 3D systems like our NPs. Therefore, the model proposed by Garcia-Otero et al. is applied here to study the magnetic properties of NPs. This model applies to magnetically isolated and 3D random particle systems.[20] It can be described as

$$H_c/H_k = 0.479 - 0.81\left(\frac{k_b T}{2K_u V}(\ln \tau_m + 20.7)\right)^{3/4} \quad (2)$$

where H_k is the critical field in Oe, defined as the field at which the NPs undergo an irreversible jump in their magnetization direction when decreasing the magnetic field, k_B the Boltzmann constant (1.38073×10^{-16} erg/K), K_u is the uniaxial anisotropy energy density in erg/cm^3, V is the particle volume in cm^3, and τ_m is the measurement time in seconds. Using this model, the magnetic properties of the magnetic NPs can be evaluated. We have plotted H_c vs $T^{3/4}$ in Figure 3c. According to eq 2, from the intercept of the H_c versus $T^{3/4}$ curves we can derive H_k. From the slopes of the curves $K_u V$ is derived.

The anisotropy constants derived from the fits with eq 2 in Figure 3c are given in Table 2. The long-range ordering parameter S for different annealing temperatures obtained based on a measured relationship between anisotropy constants K_u and ordering parameter S, is given in Table 2 as

Table 2. Anisotropy Constant K_u Derived from the Garcia-Otero Model[20] and Corresponding Long-Range Ordering Parameter S

sample	synthesis temp (°C)	synthesis time (h)	anisotropy constant K_u (10^7 erg/cm^3)	ordering parameter S (derived from K_u)
B	150	3	1.2	0.2
C	200	3	2.0	0.4
D	250	3	2.3	0.5
E	350	3	2.7	0.6

well, and plotted in Figure 3d (solid symbols).[25] The obtained ordering parameter is in good agreement with the ordering parameter determined by XRD (open symbols in Figure 3d). A large anisotropy constant underlines the potential of these NPs for high-density data storage.

Solution annealed FePtAu NPs disperse very well, indicating that the ligands are still intact. In order to demonstrate that postanneal patterning based on ligand exchange is still possible with our NPs, we have fabricated the NP patterns of Figure 4. The Si/SiO$_2$ substrate is covered with a thin (0.62 ± 0.04 nm) of hexamethyldisilazane (HMDS). Subsequently a pattern is defined by standard photolithography for selective self-assembly of the FePtAu NPs. When the substrate is dipped in the particle dispersion, pendant functional groups $-$NH$-$ of the HMDS replace the particle stabilizers and a strong NP monolayer is formed in the exposed regions. Physisorbed NPs and resist are easily removed afterward. The successful patterning of the FePtAu NPs based on ligand exchange indicates that the ligands are intact after our solution annealing procedure.

In conclusion, we have demonstrated a low-temperature solution synthesis method for fabricating FePtAu nanoparticles that remain ferromagnetic up to room temperature. Our method strongly reduces nanoparticle agglomeration associ-
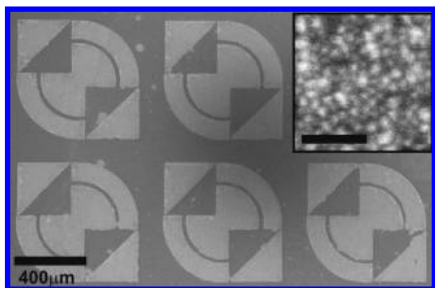
Figure 4. Scanning electron microscope (SEM) images of FePtAu NPs monolayer patterns. The insert shows a zoom-in on the patterned area. The scale bar is 50 nm.

ated with high annealing temperatures and leaves the organic ligands intact. As a result, the postannealed nanoparticles still leave the flexibility for further processing, patterning for instance. Low-temperature bottom-up synthesis of ferromagnetic, patternable nanoparticles is considered to be an important step toward application of ferromagnetic particles in high-density data storage and spintronics.

Supporting Information Available: Additional experimental details and procedures and XPS analysis of FePtAu NPs prepared via solution annealing. This material is available free of charge via the Internet at http://pubs.acs.org.

References

(1) Sun, S. H. *Adv. Mater.* **2006**, *18*, 393–403.
(2) Sun, S. H.; Murray, C. B.; Weller, D.; Folks, L.; Moser, A. *Science* **2000**, *287*, 1989–1992.
(3) Kang, S. S.; Jia, Z. Y.; Nikles, D. E.; Harrell, J. W. *IEEE Trans. Magn.* **2003**, *39*, 2753–2757.
(4) Kang, S. H.; Jia, Z. Y.; Nikles, D. E.; Harrell, J. W. *IEEE Trans. Magn.* **2004**, *40*, 513–513.
(5) Wang, S.; Kang, S. S.; Nikles, D. E.; Harrell, J. W.; Wu, X. W. *J. Magn. Magn. Mater.* **2003**, *266*, 49–56.
(6) Yu, C. H.; Caiulo, N.; Lo, C. C. H.; Tam, K.; Tsang, S. C. *Adv. Mater.* **2006**, *18*, 2312–2314.
(7) Schrefl, T.; Hrkac, G.; Suess, D.; Scholz, W.; Fidler, J. *J. Appl. Phys.* **2003**, *93*, 7041–7043.
(8) Zafiropoulou, I.; Tzitzios, V.; Petridis, D.; Devlin, E.; Fidler, J.; Hoefinger, S.; Niarchos, D. *Nanotechnology* **2005**, *16*, 1603–1607.
(9) Yamamoto, S.; Morimoto, Y.; Ono, T.; Takano, M. *Appl. Phys. Lett.* **2005**, *87*, 032503.
(10) Jones, B. A.; Dutson, J. D.; O'Grady, K.; Hickey, B. J.; Li, D. R.; Poudyal, N.; Liu, J. P. *IEEE Trans. Magn.* **2006**, *42*, 3066–3068.
(11) Momose, S.; Kodama, H.; Yamagishi, W.; Uzumaki, T. *Jpn. J. Appl. Phys., Part 2* **2007**, *46*, L1105–L1107.
(12) Kim, J.; Rong, C. B.; Lee, Y.; Liu, J. P.; Sun, S. H. *Chem. Mater.* **2008**, *20*, 7242–7245.
(13) Kim, J. M.; Rong, C. B.; Liu, J. P.; Sun, S. H. *Adv. Mater.* **2009**, *21*, 906–909.
(14) Harrell, J. W.; Nikles, D. E.; Kang, S. S.; Sun, X. C.; Jia, Z.; Shi, S.; Lawson, J.; Thompson, G. B.; Srivastava, C.; Seetala, N. V. *Scr. Mater.* **2005**, *53*, 411–416.
(15) Borchert, H.; Shevehenko, E. V.; Robert, A.; Mekis, I.; Kornowski, A.; Grubel, G.; Weller, H. *Langmuir* **2005**, *21*, 1931–1936.
(16) Warren, B. E. *X-Ray Diffraction*; Addison-Wesley Publishing Company: MA, 1969.
(17) Chepulskii, R. V.; Velev, J.; Butler, W. H. *J. Appl. Phys.* **2005**, *97*, 10J311.
(18) Jia, Z. Y.; Kang, S. S.; Nikles, D. E.; Harrell, J. W. *IEEE Trans. Magn.* **2005**, *41*, 3385–3387.
(19) Naber, W. J. M.; Faez, S.; van der Wiel, W. G. *J. Phys. D: Appl. Phys.* **2007**, *40*, R205–R228.
(20) Garcia-Otero, J.; Garcia-Bastida, A. J.; Rivas, J. *J. Magn. Magn. Mater.* **1998**, *189*, 377–383.
(21) Sun, S. H.; Anders, S.; Thomson, T.; Baglin, J. E. E.; Toney, M. F.; Hamann, H. F.; Murray, C. B.; Terris, B. D. *J. Phys. Chem. B* **2003**, *107*, 5419–5425.
(22) Chepulskii, R. V.; Butler, W. H. *Phys. Rev. B* **2005**, *72*, 134205.
(23) Klemmer, T.; Hoydick, D.; Okumura, H.; Zhang, B.; Soffa, W. A. *Scr. Metall. Mater.* **1995**, *33*, 1793–1805.
(24) Weller, D.; Moser, A. *IEEE Trans. Magn.* **1999**, *35*, 4423–4439.
(25) Shima, T.; Moriguchi, T.; Mitani, S.; Takanashi, K. *Appl. Phys. Lett.* **2002**, *80*, 288–290.

NL901465S